

TIGHT ROBUSTNESS CERTIFICATES AND WASSERSTEIN DISTRIBUTIONAL ATTACKS FOR DEEP NEURAL NETWORKS

Bach C. Le, Tung V. Dao, Binh T. Nguyen, Hong T.M. Chu

College of Engineering & Computer Science

VinUniversity

Hanoi, Vietnam

{bach.lc, tung.dv, binh.nt2, hong.ctm}@vinuni.edu.vn

ABSTRACT

Wasserstein distributionally robust optimization (WDRO) provides a framework for adversarial robustness, yet existing methods based on global Lipschitz continuity or strong duality often yield loose upper bounds or require prohibitive computation. We address these limitations with a primal approach and adopt a notion of *exact* Lipschitz certificates to tighten this upper bound of WDRO. For ReLU networks, we leverage the piecewise-affine structure on activation cells to obtain an *exact* tractable characterization of the corresponding WDRO problem. We further extend our analysis to modern architectures with smooth activations (e.g., GELU, SiLU), such as Transformers. Additionally, we propose novel Wasserstein Distributional Attacks (WDA, WDA++) that construct candidates for the worst-case distribution. Compared to existing attacks that are restricted to point-wise perturbations, our methods offer greater flexibility in the number and location of attack points. Extensive evaluations demonstrate that our proposed framework achieves competitive robust accuracy against state-of-the-art baselines while offering tighter certificates than existing methods. Our code is available at <https://github.com/OLab-Repo/WDA>

1 INTRODUCTION

Modern deep networks achieve remarkable accuracy yet remain fragile to distribution shift and adversarial perturbations Szegedy et al. (2014); Goodfellow et al. (2014); Kurakin et al. (2018); Hendrycks & Dietterich (2019); Ovadia et al. (2019); Taori et al. (2020); Koh et al. (2021), raising concerns about their reliability in deployment. A principled avenue for robustness is Wasserstein distributionally robust optimization (WDRO, Mohajerin Esfahani & Kuhn 2018; Gao & Kleywegt 2023), which controls worst-case test risk over an ambiguity set within a Wasserstein ball around the empirical distribution and admits tight dual characterizations from optimal transport (Villani et al., 2008; Santambrogio, 2015). While numerous defences have been proposed, a fundamental gap persists between theoretical robustness certificates and practical adversarial evaluation: existing Lipschitz-based certificates often provide loose upper bounds that vastly overestimate the true worst-case loss (Virmaux & Scaman, 2018), while standard attacks restrict perturbations to fixed-radius balls around individual points (Katz et al., 2017; Ehlers, 2017; Weng et al., 2018; Singh et al., 2018). This mismatch stems from two limitations: certificates typically rely on global worst-case analysis that ignores the actual network geometry traversed by data, and attacks consider only point-wise perturbations rather than distributional shifts permitted by Wasserstein threat models (Singh et al., 2018; Gao & Kleywegt, 2023). The discrepancy is particularly pronounced for modern architectures with ReLU activations, where the network behaves as a piecewise-affine function whose local properties vary dramatically across regions (Jordan & Dimakis, 2020), and those with smooth activations (GELU, SiLU/Swish) exhibit complex nonlinear geometry (Hendrycks & Gimpel, 2016; Ramachandran et al., 2017; Elfving et al., 2018). In this work, we aim to address both sides of this gap: our contributions can be summarized as follows.

1. For a class of networks with Rectified Linear Unit (ReLU) activations (Nair & Hinton, 2010), we analyse the upper and lower bounds of the Wasserstein Distributional Robust Optimization (WDRO) problem by connecting with the tight Lipschitz constant studied in Jordan & Dimakis, 2020. Our first theoretical result yields an upper bound of WDRO induced by $\mathbf{L} \triangleq 2^{1/r} \max_{\mathcal{D} \in \mathcal{D}_{\mathcal{X}}} \|J_{\mathcal{D}}\|_{r \rightarrow s}$, where $J_{\mathcal{D}}$ is general Jacobian of the logit map, see 3.1. In addition, we derive a lower bound of WDRO by constructing a concrete and finite worst-case distribution, see equation 17. This worst-case distribution is constructed by perturbing the empirical sample along the direction in which the logit map is most varied. Moreover, we provide a sufficient condition where our lower and upper bounds match, and simulate an instance to illustrate this tightness, see Figure 1. It is worth noting that not every Lipschitz constant yields a tight bound of WDRO, see Remark 3.
2. We further analyse the upper and lower bounds of the WDRO problem for a class of architectures with smooth activation and cross-entropy loss. Unlike ReLU activation or DLR loss, which might create degeneration edges, the global differentiability of smooth networks enables an exact characterization of the Lipschitz constant via the gradient norm. Similar to the analysis of the ReLU networks, we obtain the upper bound of the WDRO as $\mathbf{L} \triangleq 2^{1/r} \max_{x \in \mathcal{X}} \|\nabla \theta(x)\|_{r \rightarrow s}$ while the worst-case distribution and lower bound are constructed similar to the ReLU networks.
3. Finally, we bridge the gap between WDRO theory and adversarial evaluation by introducing the Wasserstein Distributional Attack (WDA) and its adaptive variant (WDA++), which directly constructs adversarial distributions within the Wasserstein ball rather than restricting to point-wise perturbations. Unlike existing attacks that place all adversarial examples on the ϵ -ball boundary, WDA flexibly interpolates between point-wise ($\kappa = 1$) and truly distributional attacks ($\kappa > 1$) by supporting adversarial distributions on $2N$ points, see Figure 2. WDA++ further optimizes the $2N$ -support distribution via adaptive transport budget allocation. Empirically, WDA and WDA++ consistently find stronger adversarial examples than state-of-the-art methods across diverse settings (Table 1). When integrated into the Adaptive Auto Attack framework (Liu et al., 2022), our method matches or exceeds the ensemble performance of A³. Our results demonstrate that the distributional perspective not only provides tighter theoretical certificates but also yields more effective attacks. Crucially, this exposes the limitations of current evaluation standards (e.g., AutoAttack (Croce & Hein, 2020), RobustBench (Croce et al., 2021)) which significantly overestimate robustness by restricting to Ω_{∞} rather than the larger Ω_1 ambiguity set assumed by certificates.

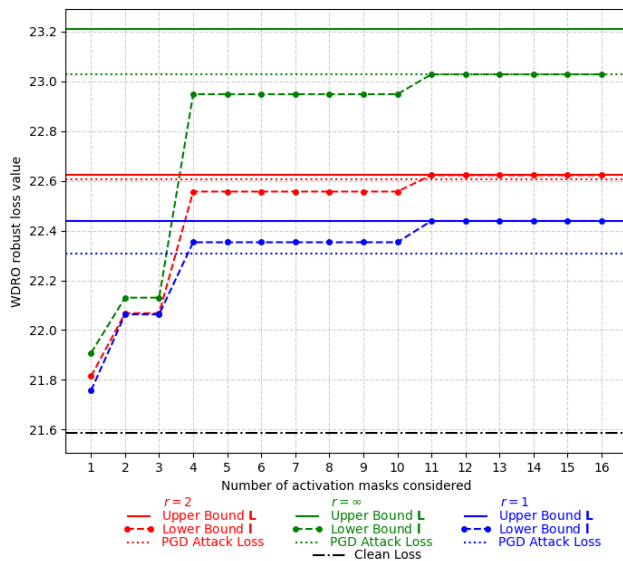


Figure 1: WDRO bounds and PGD attack loss for a ReLU classifier with $n = K = 2$ and one hidden layer of dimension 8. Lower bound curves are the cumulative l as more reachable activation masks are considered.

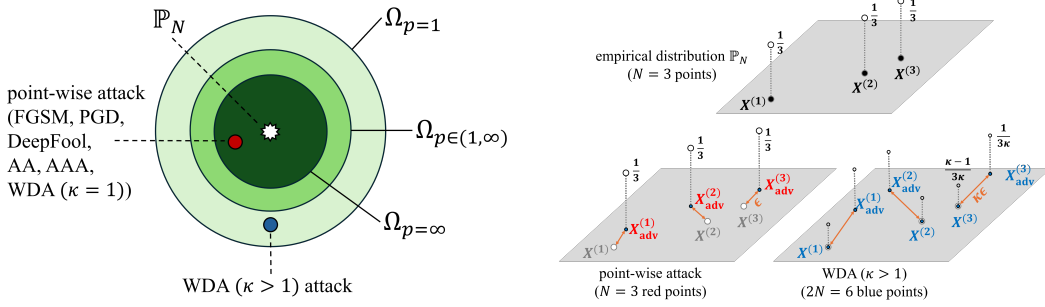


Figure 2: **Left:** Wasserstein ambiguity ball $\Omega_p = \{\mathbb{P} : \mathcal{W}_{d,p}(\mathbb{P}, \mathbb{P}_N) \leq \epsilon\}$ inclusion and its admissible attacks. Our proposed Wasserstein Distributional Attack (WDA) with $\kappa \geq 1$ includes its special case $\kappa = 1$ as a point-wise attack, and produces a distributional attack when $\kappa > 1$. Note that most of the existing tight certificates estimated an upper bound of WDRO w.r.t. $\Omega_{p=1}$, not $\Omega_{p=\infty}$. **Right:** Visualization of point-wise attack (N adversarial samples) versus our WDA ($2N$ adversarial samples). Our WDA allows not only a larger number of supports but also a wider range of perturbations.

2 PRELIMINARIES

Notations. We denote basis vector as e_k ; indicator function as $\mathbf{1}_{\{\cdot\}}$; Dirac measure as δ_z ; input dimension n , and output dimension as K . An empirical dataset is denoted $\{Z^{(1)}, \dots, Z^{(N)}\}$ with $Z = (x, y) \in \mathcal{Z} = \mathcal{X} \times \mathcal{Y}$ where $\mathcal{X} \subset \mathbb{R}^n$ and $\mathcal{Y} \subset \mathbb{R}^K$; empirical distribution $\mathbb{P}_N = \sum_i \mu_i \delta_{Z^{(i)}}$ with $Z^{(i)} = (x^{(i)}, y^{(i)}) = e_{k_i}$. Norms $\|\cdot\|_r$ and $\|\cdot\|_s$ are dual with $1/r + 1/s = 1$. For a matrix A , $\|A\|_{r \rightarrow s} = \sup_{\|u\|_r=1} \|Au\|_s$. Rectifier $(\cdot)_+ = \max\{0, \cdot\}$. Recession cone $\text{rec}(\cdot)$. Interior set $\text{int}(\cdot)$. Ground cost $d((x', y'), (x, y)) = \|x' - x\|_r + \infty \cdot \mathbf{1}_{\{y' \neq y\}}$. Cross-entropy loss $\ell(x, y; \theta) = -\sum_{k=1}^K y_k \log \text{softmax}(\theta(x))_k$. Analogous DLR loss as defined in Croce & Hein (2020). Dual-norm maximizer \mathcal{M}_r

$$\mathcal{M}_r : g \mapsto \arg \max_h \{\langle g, h \rangle \mid \|h\|_r = 1\} = \begin{cases} \text{sign}(g) & \text{if } r = \infty, \\ g/\|g\|_2 & \text{if } r = 2, \\ \text{sign}(g_{k'})e_{k'} \text{ with } k' \in \arg \max_k |g_k| & \text{if } r = 1, \end{cases} \quad (1)$$

and projector $\Pi_{r,x,R}$

$$\Pi_{r,x,R}(z) \triangleq \arg \min_{\xi} \left\{ \|\xi - z\|_2^2 \mid \|\xi - x\|_r \leq R \right\}. \quad (2)$$

WDRO. Robustness certificates aim to make model predictions trustworthy under adversarial manipulation (Wong & Kolter, 2018; Cohen et al., 2019; Salman et al., 2019). The empirical risk minimization model $\inf_{\theta} \mathbb{E}_{\mathbb{P}_N}[\ell(Z; \theta)]$ optimizes average performance on the observed data but offers no protection against worst-case shifts nearby. Distributionally robust optimization (DRO) addresses this by choosing parameters that perform well against all distributions within a prescribed neighbourhood: $\inf_{\theta} \sup_{\mathbb{P} \in \mathcal{P}} \mathbb{E}_{\mathbb{P}}[\ell(Z; \theta)]$. Here, the worst-case loss is taken over all admissible distributions $\mathbb{P} \in \mathcal{P}$. The ambiguity (or uncertainty) set \mathcal{P} is often constructed by collecting all distributions \mathbb{P} that are similar to the empirical distribution \mathbb{P}_N .

In this work, we focus on the Wasserstein ambiguity set, which is a ball centred at \mathbb{P}_N under the Wasserstein distance. Given a ground cost d on the space of data \mathcal{Z} , the Wasserstein distance $\mathcal{W}_{d,p}$ (Villani et al., 2008) between two distributions \mathbb{P} and \mathbb{Q} is defined for $p \in [1, \infty)$ as

$$\mathcal{W}_{d,p}(\mathbb{P}, \mathbb{Q}) \triangleq \left(\inf_{\pi \in \Pi(\mathbb{P}, \mathbb{Q})} \int_{\mathcal{Z} \times \mathcal{Z}} d^p(z', z) d\pi(z', z) \right)^{1/p}$$

and $\mathcal{W}_{d,p}(\mathbb{P}, \mathbb{Q}) \triangleq \inf_{\pi \in \Pi(\mathbb{P}, \mathbb{Q})} \text{ess. sup}_{\pi} (d)$ for $p = \infty$. Intuitively, the Wasserstein distance between two distributions \mathbb{P} and \mathbb{Q} is defined as the minimum cost to transport the mass of \mathbb{P} to \mathbb{Q} . The WDRO problem with a given budget of perturbation $\epsilon > 0$ can be written as

$$\inf_{\theta} \sup_{\mathbb{P} \in \Omega_p} \mathbb{E}_{\mathbb{P}}[\ell(Z; \theta)] \text{ where } \Omega_p = \{\mathbb{P} \mid \mathcal{W}_{d,p}(\mathbb{P}, \mathbb{P}_N) \leq \epsilon\}. \quad (3)$$

It is worth noting that $\mathcal{W}_{d,p} \leq \mathcal{W}_{d,p'}$ if $p \leq p'$, thus $\Omega_1 \supseteq \Omega_p \supseteq \Omega_{p'} \supseteq \Omega_\infty$ (see Figure 2). For more details on Wasserstein distributionally robust optimization, we refer reader to Kuhn et al. (2019) and our Appendix A.

Lipschitz Certificate. For $p = 1$, the worst-case risk over a Wasserstein ball admits the standard Lipschitz upper bound

$$\sup_{\mathbb{P} \in \Omega_1} \mathbb{E}_{\mathbb{P}}[\ell(Z; \theta)] \leq \mathbb{E}_{\mathbb{P}_N}[\ell(Z; \theta)] + L\epsilon. \quad (4)$$

where L is any Lipschitz constant of $z \mapsto \ell(z; \theta)$ with respect to the ground cost. This inequality follows from weak duality and is widely used to make the WDRO objective tractable: one replaces the inner maximization by the surrogate $L\epsilon$ and then controls L (Mohajerin Esfahani & Kuhn, 2018; Blanchet et al., 2019; Gao & Kleywegt, 2023; Gao et al., 2024). In practice, estimating L reduces to bounding the network’s (global or local) Lipschitz modulus, e.g., fast global products of per-layer operator norms (Virmaux & Scaman, 2018) or tighter activation-aware/local certificates (Jordan & Dimakis, 2020; Shi et al., 2022).

Adversarial Attack. Adversarial attack methods often construct a perturbed distribution by shifting each sample $X^{(i)}$ along a specific adversarial direction $u^{(i)}$ to get $X_{\text{adv}}^{(i)}$ (Goodfellow et al., 2014; Moosavi-Dezfooli et al., 2016; Carlini & Wagner, 2017). These methods are essentially point-wise attacks, which draws a distribution $\mathbb{P}_{\text{adv}} = \sum_{i=1}^N \frac{1}{N} \delta_{(X_{\text{adv}}^{(i)}, Y^{(i)})}$ in the Wasserstein ambiguity set $\Omega_p = \{\mathbb{P} : \mathcal{W}_{d,p} \leq \epsilon\}$ when $p = \infty$ (see Figure 2). Whereas, in the $p = 1$ case, the ambiguity set only constrains the average transportation cost under an optimal coupling. Hence, the adversary may move some points farther and others less as long as the mean cost stays within budget. This creates a significant gap between the robustness measured against $\Omega_{p=\infty}$ attacks and the theoretical robustness or Lipschitz certificates equation 4 which are developed for $\Omega_{p=1}$ (Mohajerin Esfahani & Kuhn, 2018; Carlini et al., 2019; Rice et al., 2021).

3 TRACTABLE INTERPRETATION OF WDRO FOR NEURAL NETWORKS

For certain shallow and convex models (e.g., linear regression, support vector machines, etc.), the tractable representation of the WDRO problem equation 3 is well-established in the literature (Mohajerin Esfahani & Kuhn, 2018; Blanchet et al., 2019; Gao & Kleywegt, 2023; Gao et al., 2024). This tractable form enables a computational advantage and provides a clear interpretation of the robustness of regularization mechanisms. In that line of work, the Lipschitz constant often provides a practical and tight upper bound of the corresponding upper bounds. However, when the loss is non-convex, the Lipschitz certificate is not always tight, as outlined in the following remark.

Remark. Consider a single-point empirical distribution $\mathbb{P}_N = \delta_{\{X^{(1)}=2\}}$ and a loss function given by

$$\ell(x) = \begin{cases} |x| & \text{if } |x| \leq 1, \\ \frac{1}{2}|x| + \frac{1}{2} & \text{otherwise.} \end{cases}$$

Then ℓ is Lipschitz with Lipschitz constant 1, however for any $\epsilon > 0$,

$$\sup_{\Omega_1} \mathbb{E}_{\mathbb{P}}[\ell(X)] = \mathbb{E}_{\mathbb{P}_N}[\ell(X)] + \frac{1}{2}\epsilon.$$

In the following, our main theoretical results (Theorems 3.1 and 3.3) show that Lipschitz modulus provides a tight upper bound for the WDRO problem equation 3 for a class of ReLU neural networks and smooth activated neural networks.

3.1 EXACT AND TRACTABLE INTERPRETATION OF WDRO FOR ReLU NEURAL NETWORKS

For a broad class of ReLU networks, the tight (local) Lipschitz constant can be found exactly via activation patterns. For example, for any H -layer ReLU network $\theta(x) = W_{H+1}(\text{ReLU}(\dots(W_1x + b_1)\dots) + b_H)$, let

$$L_\theta = \sup_{x \in \mathcal{X}} \sup_{J \in \partial\theta(x)} \|J\|_{r \rightarrow \tilde{r}}, \quad (5)$$

where $J \in \partial\theta(x)$ is a general Jacobian of θ at x , then Jordan & Dimakis (2020, Theorem 1) has shown the inequality that $\|\theta(x') - \theta(x)\|_{\tilde{r}} \leq L_\theta \times \|x' - x\|_r$ for any $x', x \in \mathcal{X}$. Moreover, if θ is in general position (Jordan & Dimakis, 2020, Definition 4), then the chain rule applies and any general Jacobian J must have a form as $W_{H+1}D_H W_H \cdots D_1 W_1$ for some $[0, 1]$ -diagonal matrix D_h , $h = 1, \dots, H$. It is worth noting that the set of ReLU networks *not* in general position is negligible (Jordan & Dimakis, 2020, Theorem 3). Now in equation 5, the maximization of a convex function (norm operator) is achieved at the vertices, thus we only need to consider 0/1-diagonal matrix D_h .

We formally introduce the concept of mask as follows.

Definition 3.1 (Mask and Cell). Let $\theta(x) = W_{H+1}(\text{ReLU}(\cdots(W_1 x + b_1) \cdots) + b_H)$ be a ReLU network which is in general position. For any tuple $\mathbf{D} = (D_1, \dots, D_H)$, we define

$$J_{\mathbf{D}} = W_{H+1}D_H W_H \cdots D_1 W_1.$$

For any $x \in \mathcal{X}$, we define the set of all 0/1-diagonal masks at x as

$$\mathcal{D}_x = \{\mathbf{D} = (D_1, \dots, D_H) \mid J_{\mathbf{D}} \in \partial\theta(x), D_h \text{ is 0/1-diagonal}, h = 1, \dots, H\}$$

We denote $\mathcal{D}_{\mathcal{X}} = \cup_{x \in \mathcal{X}} \mathcal{D}_x$ as the (finite) set of all possible masks.

For any mask $\mathbf{D} = (D_1, \dots, D_H) \in \mathcal{D}_x$, let $\mathcal{C}_{\mathbf{D}}$ be the cell, which is an open linear region, defined by

$$\mathcal{C}_{\mathbf{D}} = \{x \mid \text{pre}_h(x)_j > 0 \text{ if } D_h(j, j) = 1 \text{ and } \text{pre}_h(x)_j < 0 \text{ if } D_h(j, j) = 0, h = 1, \dots, H\},$$

where the pre-activation functions are defined as

$$\text{pre}_h: x \mapsto W_h(\text{ReLU}(\cdots(W_1 x + b_1) \cdots) + b_h).$$

Given this definition, and noting that $\mathcal{D}_{\mathcal{X}}$ is finite, one can rewrite equation 5 as $L_\theta = \max_{\mathbf{D} \in \mathcal{D}_{\mathcal{X}}} \|J_{\mathbf{D}}\|_{r \rightarrow \tilde{r}}$. We adopt this notion and show that it induces an upper bound for the Wasserstein distributional robust optimization (WDRO) problem equation 3 with cross-entropy loss. Moreover, this upper bound is tight for a class of monotonic ReLU networks.

Theorem 3.1 (WDRO for ReLU Networks). *Given a ReLU network*

$$\theta(x) = W_{H+1}(\text{ReLU}(\cdots(W_1 x + b_1) \cdots) + b_H)$$

being in general position, $1/r + 1/s = 1$ and ℓ being the cross-entropy or DLR loss, define

$$\mathbf{L} \triangleq 2^{1/r} \max_{\mathbf{D} \in \mathcal{D}_{\mathcal{X}}} \|J_{\mathbf{D}}\|_{r \rightarrow s}, \quad (6)$$

and

$$\mathbf{l} \triangleq \max_{\substack{x \in \mathcal{X}, \\ \mathbf{D} \in \mathcal{D}_x}} \max_{k' \neq k} \sup_{\|u\|_r=1} \{(e_{k'} - e_k)^\top J_{\mathbf{D}} u \mid u \in \text{rec}(\mathcal{C}_{\mathbf{D}})\}. \quad (7)$$

where $J_{\mathbf{D}}$, $\mathcal{C}_{\mathbf{D}}$, $\mathcal{D}_{\mathcal{X}}$ are defined in Definition 3.1 and $\text{rec}(\mathcal{C}_{\mathbf{D}})$ is the recession cone of $\mathcal{C}_{\mathbf{D}}$. Then for any $\epsilon > 0$, we have

$$\mathbb{E}_{\mathbb{P}_N}[\ell(Z; \theta)] + \mathbf{l}\epsilon \leq \sup_{\mathbb{P}: \mathcal{W}_{d,1}(\mathbb{P}, \mathbb{P}_N) \leq \epsilon} \mathbb{E}_{\mathbb{P}}[\ell(Z; \theta)] \leq \mathbb{E}_{\mathbb{P}_N}[\ell(Z; \theta)] + \mathbf{L}\epsilon. \quad (8)$$

Moreover, let \mathbf{D}^* be a maximizer of equation 6, (k'^*, k^*) be a maximizer of equation 7 and $(e_{k'^*} - e_{k^*})$ be the largest increment direction of $J_{\mathbf{D}^*}$. If the dual-norm maximizer $\mathcal{M}_r(J_{\mathbf{D}^*}^\top (e_{k'^*} - e_{k^*})) \in \text{rec}(\mathcal{C}_{\mathbf{D}^*})$ then $\mathbf{l} = \mathbf{L}$.

Proof. To prove inequality equation 8, we show that the loss function $\ell(\cdot, \theta)$ is \mathbf{L} -Lipschitz, and a direction u found in equation 7 induces an admissible attack distribution \mathbb{P}_{adv} satisfying $\mathbb{E}_{\mathbb{P}_{\text{adv}}}[\ell(Z; \theta)] \approx \mathbb{E}_{\mathbb{P}_N}[\ell(Z; \theta)] + \mathbf{l}\epsilon$, $\mathcal{W}_{d,1}(\mathbb{P}_{\text{adv}}, \mathbb{P}_N) \leq \epsilon$. To verify the sufficient condition of $\mathbf{l} = \mathbf{L}$, we show that the constructed \mathbb{P}_{adv} provides $\mathbf{l} = \mathbf{L}$. We provide detailed proof in Appendix B.1. \square

In Figure 1, we illustrate an instance in which our lower and upper bounds match. While equation 7 provides a tight lower bound of the WDRO, it is impractical to scan through all $x \in \mathcal{X}$ and its mask \mathcal{D}_x . We then introduce a practical lower bound, of which we consider the mask associated with the sample points only.

Corollary 3.2 (Practical lower bound). *Given assumptions and notations used in Theorem 3.1, let $\mathcal{Z}_N = \{(X^{(1)}, Y^{(1)}), \dots, (X^{(N)}, Y^{(N)})\}$ and*

$$l_N \triangleq \max_{\substack{(X^{(i)}, Y^{(i)}) \in \mathcal{Z}_N \\ D \in \mathcal{D}_x}} \max_k \sup_{\|u\|_r=1} \left\{ (e_k - Y^{(i)})^\top J_D u \mid u \in \text{int}(\text{rec}(\mathcal{C}_D)) \right\}. \quad (9)$$

Then $l_N \leq l$.

Based on the proof of our lower bound equation 17, we construct a worst-case distribution by moving mass from a sample along a direction u that maximizes the margin term in equation 7. In Section 4, based on formulation equation 9, we create this construction empirically via the attack distribution equation 11 by choosing adversarial direction $u^{(i)}$ for each sample i so that it maximizes the first-order increase of the corresponding logit margin.

3.2 EXACT AND TRACTABLE INTERPRETATION OF WDRO FOR SMOOTH ACTIVATION NEURAL NETWORKS

While ReLU networks require analyses of activation masks, modern architectures often employ smooth activation functions (e.g., GELU (Hendrycks & Gimpel, 2016), SiLU (Ramachandran et al., 2017)). In these settings, the WDRO duality connects the worst-case adversarial risk directly to the first-order geometry via the Jacobian of the logit map.

Theorem 3.3 (WDRO for Smooth Networks). *Given a differentiable network $\theta : \mathbb{R}^n \rightarrow \mathbb{R}^K$ with $J_\theta(x) \in \mathbb{R}^{K \times n}$ being its Jacobian, $1/r + 1/s = 1$ and ℓ being the cross-entropy or DLR loss, define*

$$\mathbf{L} \triangleq 2^{1/r} \sup_{x \in \mathcal{X}} \|J_\theta(x)\|_{r \rightarrow s},$$

and

$$l \triangleq \sup_{x \in \mathcal{X}} \max_{k' \neq k} \sup_{\|u\|_r=1} (e_{k'} - e_k)^\top J_\theta(x) u.$$

Then for any $\epsilon > 0$,

$$\mathbb{E}_{\mathbb{P}_N}[\ell(Z; \theta)] + l\epsilon \leq \sup_{\mathbb{P}: \mathcal{W}_{d,1}(\mathbb{P}, \mathbb{P}_N) \leq \epsilon} \mathbb{E}_{\mathbb{P}}[\ell(Z; \theta)] \leq \mathbb{E}_{\mathbb{P}_N}[\ell(Z; \theta)] + \mathbf{L}\epsilon.$$

In addition, this result extends certification guarantees to modern differentiable Transformer architectures such as GPT (Radford et al., 2019), ViT (Dosovitskiy et al., 2021), and Swin Transformer (Liu et al., 2021), which are often Pre-LN Transformers Xiong et al. (2020).

Corollary 3.4 (WDRO for Pre-LN Transformers). *Given assumptions and notations used in Theorem 3.3, if θ is a depth- H (Pre-LN) Transformer, then by Castin et al. (2024, Theorem 3.3 and Lemma 3.8), the upper bound satisfies*

$$\mathbf{L} = 2^{1/r} \sup_{x \in \mathcal{X}} \|J_\theta(x)\|_{r \rightarrow s} \leq 2^{1/r} (nK)^{\left(\frac{1}{2} - \frac{1}{r}\right)_+} \times \Lambda_\theta, \quad (10)$$

where $\Lambda_\theta \triangleq L_{\text{head}} L_{\text{emb}} \prod_{h=1}^H \left(1 + L_{\text{LN}}^{(h)} L_{\text{MHA}}^{(h)}\right) \left(1 + L_{\text{LN}'}^{(h)} L_{\text{FFN}}^{(h)}\right)$, and all module constants are Euclidean Lipschitz constants on \mathcal{X} . Moreover, their explicit bound of the form $L_{\text{MHA}}^{(h)} = \mathcal{O}(\sqrt{n})$ implies $\mathbf{L} = \mathcal{O}\left(2^{1/r} (nK)^{\left(\frac{1}{2} - \frac{1}{r}\right)_+} \times n^{H/2}\right)$ up to architecture and parameter-dependent constants.

4 WASSERSTEIN DISTRIBUTIONAL ATTACKS

Existing point-wise attacks such as FGSM (Goodfellow et al., 2014), DeepFool (Moosavi-Dezfooli et al., 2016), AA (Croce & Hein, 2020), AAA (Liu et al., 2022), keep the adversarial distribution supported on exactly N points, where each point $X_{\text{adv}}^{(i)}$ is perturbed to be precisely on the boundary of the ϵ -ball centred at $X^{(i)}$. To address this issue, we propose a novel method called *Wasserstein Distributional Attacks* which constructs an adversarial distribution \mathbb{P}_{adv} , supported on a set of $2N$ label-preserving points

$$\mathbb{P}_{\text{adv}} = \frac{1}{N} \sum_{i=1}^N \left(1 - \frac{1}{\kappa_i}\right) \delta_{(X^{(i)}, Y^{(i)})} + \frac{1}{\kappa_i} \delta_{(X_{\text{adv}}^{(i)}, Y^{(i)})}, \quad (11)$$

where $\kappa_i \geq 1$. (See Figure 2.) This $2N$ -support consists of N original empirical samples $X^{(i)}$ and N corresponding adversarial points $X_{\text{adv}}^{(i)}$, each perturbed using the first-order, margin-aligned directions predicted by Theorems 3.1 and 3.3.

WDA. WDA corresponds to $\kappa_i \equiv \kappa$. In the special case where $\kappa = 1$, the attack reduces to point-wise methods, while $\kappa = 2$ yields a uniform distribution over all $2N$ points, with each point receiving a weight of $\frac{1}{2N}$. The mixture equation 11 lies in Ω_p whenever $\|X_{\text{adv}}^{(i)} - X^{(i)}\|_r \leq \kappa^{1/p} \epsilon$ for all i (Corollary C.2) and serves as a constructive and feasible distributional adversary.

WDA++. WDA++ keeps the same two-point anchored form equation 11 but chooses the mixing weight adaptively. For each sample i we calculate d_i , an estimate of the closest distance to flip an image’s label and set $1/\kappa_i = \min\{1, t_i/d_i^p\}$ for a transport allocation $t_i \geq 0$ (with the conventions $1/\kappa_i = 1$ if $d_i = 0$ and $1/\kappa_i = 0$ if $d_i = \infty$), yielding $X_{\text{adv}}^{(i)}$ chosen near the closest flip. By Corollary C.2, $\mathcal{W}_{d,p}(\mathbb{P}_{\text{adv}}, \mathbb{P}_N)^p \leq \sum_i \mu_i t_i$, hence $\mathbb{P}_{\text{adv}} \in \Omega_p$ whenever $\sum_i \mu_i t_i \leq \epsilon^p$. Full implementation details are deferred to Appendix E.

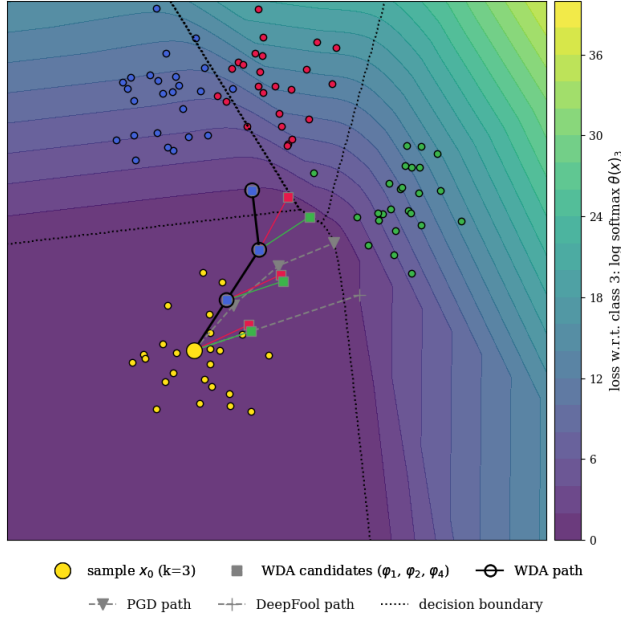


Figure 3: Wasserstein Distributional Attack (WDA, Algorithm 1) for $r = 2$. At each iteration x_t , WDA forms $K - 1$ candidates φ_j and updates using the one with the largest logit $\theta_j(\varphi_j)$. For reference, PGD follows the dual-norm gradient direction; DeepFool linearizes the decision boundary.

Adversarial direction. Define the (sub)gradient $g_j(x) \in \partial_x(\theta_j - \theta_k)(x)$. Then $\mathcal{M}_r(g_j)$ provides the per-iteration, first-order instance of the ray ascent from Theorems 3.1 and 3.3: within a ReLU cell or for smooth activations, moving along $u_j = \mathcal{M}_r(g_j)$ increases the gap at rate $\|g_j(x)\|_s$. During an initial probing phase, we evaluate all rivals $j \neq k$ using these first-order steps. At the end of this phase, we fix a single rival j^* based on the logit magnitude and continue the remaining iterations. Fixating j^* prevents the update from oscillating across classes or chasing locally steep but globally suboptimal directions. Finally, we project each step to the ball of radius $\kappa^{1/p} \epsilon$ around the anchor $X^{(i)}$. A visualization of our algorithm is shown in Figure 3. The procedures for implementing WDA and WDA++ are presented in Algorithms 1 and 2.

Algorithm 1 Wasserstein Distributional Attack (WDA)

Inputs: neural network $\theta : \mathbb{R}^n \rightarrow \mathbb{R}^K$, empirical distribution $\mathbb{P}_N = \frac{1}{N} \sum_{i=1}^N \delta_{(X^{(i)}, Y^{(i)})}$, budget $\epsilon > 0$, cost-norm $r \in \{1, 2, \infty\}$, Wasserstein order $p \in \{1, 2\}$, WDA parameter $\kappa \geq 1$, step size $\alpha > 0$, and $0 < \text{probe} \leq \text{maxiter}$

Outputs: Wasserstein distributional attack \mathbb{P}_{adv} such that $\mathcal{W}_{d,p}(\mathbb{P}_{\text{adv}}, \mathbb{P}_N) \leq \epsilon$ where $d((x', y'), (x, y)) = \|x' - x\|_r + \infty \cdot \mathbf{1}_{\{y' \neq y\}}$

Initialize: dual-norm maximizer \mathcal{M} equation 1, projection Π equation 2

for $i = 1$ to N **do**

$x_0 \leftarrow X^{(i)}, e_k \leftarrow Y^{(i)}$ for some $k = 1, \dots, K$

for $\text{iter} = 0$ to maxiter **do**

if $\text{iter} < \text{probe}$ **then** $\mathcal{J} = \{1, \dots, K\} \setminus \{k\}$ **else** $\mathcal{J} = \{j^*\}$

$g_j \leftarrow \nabla_x \theta(x_{\text{iter}})^\top (e_j - e_k)$ for $j \in \mathcal{J}$

$u_j \leftarrow \mathcal{M}_r(g_j)$ for $j \in \mathcal{J}$

$\varphi_j \leftarrow \Pi_{r, X^{(i)}, \kappa^{1/p} \epsilon}(x_{\text{iter}} + \alpha u_j)$ for $j \in \mathcal{J}$

$j^* \leftarrow \arg \max_{j \in \mathcal{J}_i} (\theta_j(\varphi_j) - \theta_k(\varphi_j))$

$x_{\text{iter}+1} \leftarrow \varphi_{j^*}$

end for

$X_{\text{adv}}^{(i)} \leftarrow x_{\text{maxiter}}$

end for

$\mathbb{P}_{\text{adv}} \leftarrow \frac{1}{N} \sum_{i=1}^N (1 - \frac{1}{\kappa}) \delta_{(X^{(i)}, Y^{(i)})} + \frac{1}{\kappa} \delta_{(X_{\text{adv}}^{(i)}, Y^{(i)})}$

return \mathbb{P}_{adv}

5 RELATED WORK

Robustness certificates. Early scalable global certificates control the Lipschitz constant by multiplying per-layer operator norms, which is fast to compute yet data-agnostic and typically loose on deep nets (Virmaux & Scaman, 2018). For ReLU networks, local (activation-aware) methods exploit piecewise linearity to produce much tighter, input-conditioned certificates on individual activation regions (Katz et al., 2017; Ehlers, 2017; Weng et al., 2018; Singh et al., 2018; Shi et al., 2022). Most relevant to exact local Lipschitzness, Jordan & Dimakis (2020) showed that for a broad class of ReLU networks in general position, the local Lipschitz constant can be computed exactly by optimizing over activation patterns.

Adversarial attacks. Adversarial Attack methods seek for perturbation x' formed by adding a small, human-imperceptible perturbation to a clean input x that causes misclassification (Szegedy et al., 2014). The threat model specifies the attacker’s knowledge (white-box vs. black-box), the admissible perturbation set (e.g., r_2 balls with budget ϵ), and the objective (e.g., worst-case loss within the ball). Canonical white-box methods include FGSM (Goodfellow et al., 2014), multistep PGD (Madry et al., 2018), CW (Carlini & Wagner, 2017), and gradient-based margin attacks such as DeepFool (Moosavi-Dezfooli et al., 2016). In the context of distributional threats, Bai et al. (2023) introduced W-PGD which transports the empirical measure while maintaining its support size. This effectively restricts the attack to a point-wise one. Our work adopts a different perspective by expanding the support to $2N$ points, thereby exploring a larger region of the ambiguity set. Decision-based and score-free attacks (black-box) include Boundary Attack (Brendel et al., 2021) and Square Attack (Andriushchenko et al., 2020).

Robust evaluation is subtle: gradient masking can inflate apparent robustness if attacks are not adapted (Athalye et al., 2018). To standardize evaluation, AutoAttack (AA) (Croce & Hein, 2020) composes strong, parameter-free attacks (APGD-CE, APGD-DLR, FAB, Square) and is widely adopted for reporting robust accuracy. RobustBench (Croce et al., 2021) curates model zoos and standardized test protocols across datasets and r_p threat models, enabling comparable and reproducible robustness claims. Liu et al. (2022) proposed Adaptive Auto Attack (A^3), which incorporates Adaptive Direction Initialization (ADI) and Online Statistics-based Discarding (ODS) (Tashiro et al., 2020) with a PGD framework to enhance attack efficiency. In our experiments, we report robustness under AA and A^3 following RobustBench conventions and use them as baselines for comparison.

Several works have focused on adversarial attacks tailored to ReLU networks. Croce & Hein (2018) introduced rLR-QP, a gradient-free method that navigates the piecewise-linear regions of ReLU

models by solving convex subproblems and enhancing exploration with randomization and local search. More recently, Zhang et al. (2022) developed BaB-Attack, a branch-and-bound framework that operates in activation space, leveraging bound propagation, beam search, and large neighborhood search to uncover stronger adversarial examples than conventional gradient-based approaches, particularly on hard-to-attack inputs. As pointed out in Zhang et al. (2022); Croce et al. (2020), rLR-QP and BaB-Attack are not as efficient as gradient based attack, therefore, for single method (Ω_∞) baseline we only use APGD.

6 COMPARISON WITH EXISTING BASELINES

Experimental setup. We evaluate the effectiveness of WDA and WDA++ in amplifying misclassification rates against state-of-the-art defences on CIFAR-10, CIFAR-100, and ImageNet. We report robustness under r_∞ and r_2 perturbations with budgets $\epsilon \in \{4/255, 8/255, 0.5\}$. Defence models and pre-trained weights are sourced from RobustBench (Croce et al., 2021). Our benchmarks include single-method baselines (APGD-CE, APGD-DLR, W-PGD) and ensemble methods (AA, A³).

For baselines, we copy the official default configurations.

For WDA, we use probe steps `probe` = 10, attack iterations `max_iter` = 20 and step size $\alpha = 0.2$ for $r_2, \epsilon = 0.5, \alpha \in \{0.01, 0.02\}$ for $r_\infty, \epsilon \in \{4/255, 8/255\}$ respectively. We further propose A³-WDA, an extension that substitutes the PGD attack of A³ with our WDA attack. In addition to standard point-wise evaluation with $\kappa = 1$, we validate the distributional threat model using $\kappa = 2$. We report the classification accuracy on the constructed distribution \mathbb{P}_{adv} as $(1 - 1/\kappa) \times \text{acc}_{\text{clean}} + (1/\kappa) \times \text{acc}_{\text{adv}}$. Comprehensive ablation studies are detailed in Appendix D.

For WDA++, we evaluate under the constrained Ω_2 set (comparable to W-PGD) and the full Wasserstein ambiguity ball Ω_1 . We adopt the parameter settings of WDA and detail the implementation in Appendix E.

All experiments are conducted on 2x NVIDIA GeForce RTX 4090 and 1x NVIDIA H200 GPUs.

Results on CIFAR-10. Table 1 presents performance on CIFAR-10. Under both r_∞ and r_2 threat models, WDA++ (Ω_1) significantly reduces robust accuracy compared to all other methods. This confirms that standard robustness benchmarks significantly overestimate true robustness against distributional shifts. Moreover, expanding the ambiguity set to the full Wasserstein ball (Ω_1) exposes vulnerabilities that both distributional adversaries under Ω_2 and point-wise attacks under Ω_∞ fail to detect. Within the Ω_2 constraint, WDA++ produces lower robust accuracy compared to W-PGD, confirming that our attack finds better directions in the loss landscape and utilises the Wasserstein budget ϵ more efficiently. Within the point-wise setting ($\kappa = 1$), WDA remains competitive, outperforming single-method attacks (APGD-CE and APGD-DLR) and achieves results comparable to ensemble-based methods, indicating its ability to match the strength of more computationally demanding attack aggregations. When integrated into the ensemble framework (A³-WDA), our method consistently achieves the lowest robust accuracy, surpassing the standard A³ and AA benchmarks.

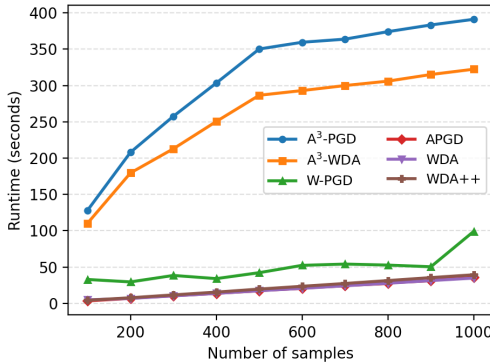
Results on CIFAR-100 and ImageNet. The dominance of WDA++ generalizes to larger-scale datasets. On CIFAR-100, while point-wise WDA ($\kappa = 1$) remains competitive against APGD variants, WDA++ (Ω_1) proves most effective, yielding the lowest single-method robustness. This trend continues on ImageNet, where WDA++ (Ω_1) outperforms all baselines, demonstrating that the full distributional threat model offers the strongest evaluation of model robustness across architectures. Finally, the ensemble A³-WDA consistently sets the state-of-the-art benchmark among ensemble methods.

Runtime comparison. Figure 4a benchmarks the scalability of the WDA framework against PGD baselines on ImageNet, exhibiting a linear relationship between runtime and sample size across all methods. WDA variants consistently maintain comparable or lower computational costs than their PGD counterparts.

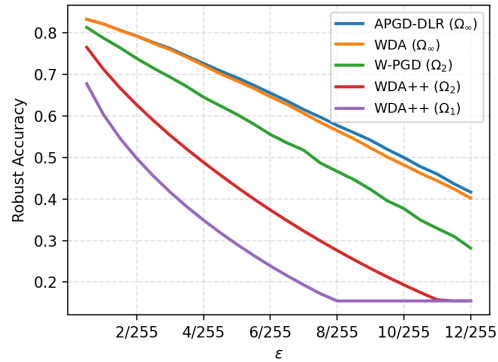
Table 1: Comparison of robust accuracy of WDA and baseline methods against various defences on CIFAR-10, CIFAR-100 and ImageNet. The best (lowest) robust accuracy of single methods and ensemble methods are highlighted in underline and **bold**, respectively.

| PAPER | MODEL | CLEAN | SINGLE METHOD | | | | | | ENSEMBLE METHOD | | | | |
|---|-------------------|-------|---------------------|--------------|------------|---------------------|-----------------|------------|-----------------|---------------------|-------|-----------------------|-----------------------|
| | | | Ω_1 | | Ω_2 | | Ω_∞ | | Ω_∞ | | | | |
| | | | WDA $\kappa = 2$ | WDA++ | W-PGD | WDA $\kappa = 2$ | WDA++ | APGD CE | APGD DLR | WDA $\kappa = 1$ | AA | A ³ PGD | A ³ WDA |
| CIFAR-10 - $r_\infty, \epsilon = 8/255$ | | | | | | | | | | | | | |
| BARTOLDSON ET AL. 2024 | WRN-94-16 | 93.68 | 65.25 | <u>32.90</u> | 58.71 | 77.09 | 46.46 | 76.15 | 74.31 | 74.05 | 73.71 | 73.55 | 73.54 |
| BARTOLDSON ET AL. 2024 | WRN-82-8 | 93.11 | 62.06 | <u>27.79</u> | 56.81 | 75.33 | 41.60 | 74.17 | 72.54 | 71.85 | 71.59 | 71.46 | 71.46 |
| CUI ET AL. 2024 | WRN-28-10 | 92.16 | 60.01 | <u>26.39</u> | 50.97 | 72.61 | 39.18 | 70.60 | 68.62 | 68.07 | 67.73 | 67.58 | 67.57 |
| WANG ET AL. 2023 | WRN-70-16 | 93.25 | 63.08 | <u>28.60</u> | 55.17 | 74.80 | 41.80 | 73.46 | 71.68 | 71.02 | 70.69 | 70.53 | 70.52 |
| WANG ET AL. 2023 | WRN-28-10 | 92.44 | 60.96 | <u>23.81</u> | 52.03 | 72.67 | 36.91 | 70.24 | 68.24 | 67.60 | 67.31 | 67.17 | 67.17 |
| XU ET AL. 2023 | WRN-28-10 | 93.69 | 63.25 | <u>36.27</u> | 52.48 | 73.98 | 46.04 | 67.08 | 69.00 | 66.39 | 63.89 | 63.93 | 63.84 |
| SEHWAG ET AL. 2022 | RN-18 | 84.59 | 54.65 | <u>15.23</u> | 46.58 | 63.86 | 27.38 | 58.40 | 57.66 | 56.30 | 55.54 | 55.50 | 55.50 |
| CIFAR-10 - $r_2, \epsilon = 0.5$ | | | | | | | | | | | | | |
| WANG ET AL. 2023 | WRN-70-16 | 95.54 | 77.63 | <u>55.57</u> | 70.09 | 86.37 | 66.73 | 85.66 | 85.30 | 85.00 | 84.97 | 84.96 | 84.97 |
| WANG ET AL. 2023 | WRN-28-10 | 95.16 | 76.31 | <u>57.42</u> | 68.65 | 85.33 | 68.10 | 84.52 | 83.89 | 83.71 | 83.68 | 83.68 | 83.68 |
| SEHWAG ET AL. 2022 | WRN-34-10 | 90.93 | 72.01 | <u>39.25</u> | 67.96 | 79.87 | 53.13 | 78.23 | 78.16 | 77.51 | 77.24 | 77.22 | 77.25 |
| SEHWAG ET AL. 2022 | RN-18 | 89.76 | 69.75 | <u>48.40</u> | 65.02 | 77.68 | 58.64 | 75.24 | 75.32 | 74.69 | 74.41 | 74.41 | 74.40 |
| DING ET AL. 2020 | WRN-28-4 | 88.02 | 63.04 | <u>31.35</u> | 53.47 | 71.61 | 42.89 | 66.62 | 66.62 | 66.22 | 66.09 | 66.05 | 66.06 |
| RONY ET AL. 2019 | WRN-28-10 | 89.05 | 64.19 | <u>27.79</u> | 51.15 | 72.30 | 39.94 | 66.58 | 67.08 | 66.59 | 66.44 | 66.41 | 66.42 |
| CIFAR-100 - $r_\infty, \epsilon = 8/255$ | | | | | | | | | | | | | |
| CUI ET AL. 2024 | WRN-28-10 | 73.85 | 43.68 | <u>6.71</u> | 24.64 | 50.42 | 10.85 | 43.82 | 40.37 | 39.57 | 39.18 | 39.17 | 39.14 |
| WANG ET AL. 2023 | WRN-28-10 | 72.58 | 43.61 | <u>7.45</u> | 24.90 | 49.81 | 10.88 | 44.09 | 39.66 | 39.12 | 38.77 | 38.70 | 38.71 |
| ADDEPALLI ET AL. 2022 | RN-18 | 65.45 | 37.64 | <u>3.07</u> | 14.52 | 42.01 | 7.80 | 33.47 | 28.82 | 28.26 | 27.67 | 27.65 | 27.63 |
| IMAGENET - $r_\infty, \epsilon = 4/255$ | | | | | | | | | | | | | |
| XU ET AL. 2025 | SWIN-L | 78.62 | 54.86 | <u>17.96</u> | 48.68 | 62.09 | 30.96 | 59.96 | 60.30 | 58.00 | 59.68 | 58.32 | 58.30 |
| AMINI ET AL. 2025 | MEANSPARSE SWIN-L | 78.80 | 59.83 | <u>25.25</u> | 54.56 | 65.28 | 38.35 | 62.12 | 62.54 | 61.14 | 58.92 | 58.76 | 58.76 |
| LIU ET AL. 2025 | CONVNEXT-B | 76.02 | 52.95 | <u>16.23</u> | 45.84 | 59.79 | 28.46 | 55.90 | 56.78 | 54.38 | 55.82 | 53.19 | 53.18 |
| SINGH ET AL. 2023 | CVNEXT-S-CVST | 74.10 | 50.31 | <u>12.06</u> | 41.40 | 56.35 | 23.97 | 52.82 | 53.20 | 51.04 | 52.42 | 49.92 | 49.90 |

Epsilon effect. Figure 4b demonstrates that WDA++ degrades performance faster than W-PGD as ϵ increases. This stems from W-PGD’s suboptimal use of global projection, which uniformly rescales perturbations and allows high-cost samples to dilute the budget. In contrast, WDA++ employs a searching method that prioritizes cheaper samples, saving budget from hard-to-attack inputs to facilitate larger, necessary perturbations on vulnerable ones.



(a) Runtime comparison of different algorithms on the ImageNet dataset.



(b) Robust accuracy of Sehwaq et al. (2022)’s ResNet-18 on CIFAR-10 under increasing ϵ .

7 CONCLUSIONS

We presented tight robustness certificates and stronger adversarial attacks for deep neural networks by exploiting their local geometric structure. For ReLU networks, we derived exact WDRO bounds using their piecewise-affine property, computing data-dependent Lipschitz constants from activation patterns that significantly tighten existing global bounds. For networks with smooth activations (e.g., GELU, SiLU), we characterized the worst-case loss through asymptotic Jacobian behavior along adversarial rays, providing the first tractable WDRO analysis for these modern architectures. Our Wasserstein Distributional Attacks (WDA, WDA++) construct adversarial distributions on $2N$ points rather than restricting to N perturbed points, achieving lower robust accuracy than state-of-the-art methods across CIFAR-10/100 and ImageNet benchmarks. While WDA and WDA++ incur

additional computational overhead compared to single-point attacks due to evaluating multiple candidate perturbations per iteration, it demonstrates that existing robustness evaluations significantly underestimate vulnerability by considering only point-wise perturbations. Together, these contributions narrow the gap between theoretical certificates and practical evaluation, revealing that both tighter bounds and stronger attacks emerge from properly leveraging network geometry and distributional perspectives.

REFERENCES

- Sravanti Addepalli, Samyak Jain, et al. Efficient and effective augmentation strategy for adversarial training. *Advances in Neural Information Processing Systems*, 35:1488–1501, 2022.
- Sajjad Amini, Mohammadreza Teymorianfard, Shiqing Ma, and Amir Houmansadr. Meansparse: Post-training robustness enhancement through mean-centered feature sparsification. *arXiv preprint arXiv:2406.05927*, 2025.
- Maksym Andriushchenko, Francesco Croce, Nicolas Flammarion, and Matthias Hein. Square attack: a query-efficient black-box adversarial attack via random search. In *European conference on computer vision*, pp. 484–501. Springer, 2020.
- Anish Athalye, Nicholas Carlini, and David Wagner. Obfuscated gradients give a false sense of security: Circumventing defenses to adversarial examples. In *International conference on machine learning*, pp. 274–283. PMLR, 2018.
- Xingjian Bai, Yifan Jiang, Guangyi He, and Jan Obłój. Wasserstein distributional robustness of neural networks. In *Advances in Neural Information Processing Systems*, volume 36, pp. 64972–64986, 2023.
- Brian R Bartoldson, James Diffenderfer, Konstantinos Parasyris, and Bhavya Kailkhura. Adversarial robustness limits via scaling-law and human-alignment studies. In *Proceedings of the 41st International Conference on Machine Learning*, pp. 3046–3072, 2024.
- Jose Blanchet, Yang Kang, and Karthyek Murthy. Robust wasserstein profile inference and applications to machine learning. *Journal of Applied Probability*, 56(3):830–857, 2019.
- Wieland Brendel, Jonas Rauber, Matthias Bethge, and Decision-Based Adversarial. Decision-based adversarial attacks: Reliable attacks against black-box machine learning models. *Advances in Reliably Evaluating and Improving Adversarial Robustness*, pp. 77, 2021.
- Nicholas Carlini and David Wagner. Towards evaluating the robustness of neural networks. In *2017 IEEE Symposium on Security and Privacy (SP)*, pp. 39–57. IEEE, 2017.
- Nicholas Carlini, Anish Athalye, Nicolas Papernot, Wieland Brendel, Jonas Rauber, Dimitris Tsipras, Ian Goodfellow, Aleksander Madry, and Alexey Kurakin. On evaluating adversarial robustness. *arXiv preprint arXiv:1902.06705*, 2019.
- Valérie Castin, Pierre Ablin, and Gabriel Peyré. How smooth is attention? In *International Conference on Machine Learning*, pp. 5817–5840. PMLR, 2024.
- Hong Chu, Meixia Lin, and Kim-Chuan Toh. Wasserstein distributionally robust optimization and its tractable regularization formulations. *arXiv preprint arXiv:2402.03942*, 2024.
- Jeremy Cohen, Elan Rosenfeld, and Zico Kolter. Certified adversarial robustness via randomized smoothing. In *International Conference on Machine Learning*, pp. 1310–1320. PMLR, 2019.
- Francesco Croce and Matthias Hein. A randomized gradient-free attack on relu networks. In *German Conference on Pattern Recognition*, pp. 215–227. Springer, 2018.
- Francesco Croce and Matthias Hein. Reliable evaluation of adversarial robustness with an ensemble of diverse parameter-free attacks. In *International Conference on Machine Learning*, pp. 2206–2216. PMLR, 2020.

- Francesco Croce, Jonas Rauber, and Matthias Hein. Scaling up the randomized gradient-free adversarial attack reveals overestimation of robustness using established attacks. *International Journal of Computer Vision*, 128(4):1028–1046, 2020.
- Francesco Croce, Maksym Andriushchenko, Vikash Sehwal, Edoardo Debenedetti, Nicolas Flammarion, Mung Chiang, Prateek Mittal, and Matthias Hein. Robustbench: a standardized adversarial robustness benchmark. In *Thirty-fifth Conference on Neural Information Processing Systems Datasets and Benchmarks Track (Round 2)*, 2021.
- Jiequan Cui, Zhuotao Tian, Zhisheng Zhong, Xiaojuan Qi, Bei Yu, and Hanwang Zhang. Decoupled kullback-leibler divergence loss. *Advances in Neural Information Processing Systems*, 37:74461–74486, 2024.
- Gavin Weiguang Ding, Yash Sharma, Kry Yik Chau Lui, and Ruitong Huang. Mma training: Direct input space margin maximization through adversarial training. In *International Conference on Learning Representations*, 2020.
- Alexey Dosovitskiy, Lucas Beyer, Alexander Kolesnikov, Dirk Weissenborn, Xiaohua Zhai, Thomas Unterthiner, Mostafa Dehghani, Matthias Minderer, Georg Heigold, Sylvain Gelly, et al. An image is worth 16x16 words: Transformers for image recognition at scale. In *International Conference on Learning Representations*, 2021.
- Ruediger Ehlers. Formal verification of piece-wise linear feed-forward neural networks. In *International Symposium on Automated Technology for Verification and Analysis*, pp. 269–286. Springer, 2017.
- Stefan Elfving, Eiji Uchibe, and Kenji Doya. Sigmoid-weighted linear units for neural network function approximation in reinforcement learning. *Neural Networks*, 107:3–11, 2018.
- Rui Gao and Anton Kleywegt. Distributionally robust stochastic optimization with wasserstein distance. *Mathematics of Operations Research*, 48(2):603–655, 2023.
- Rui Gao, Xi Chen, and Anton J Kleywegt. Wasserstein distributionally robust optimization and variation regularization. *Operations Research*, 72(3):1177–1191, 2024.
- Ian J. Goodfellow, Jonathon Shlens, and Christian Szegedy. Explaining and harnessing adversarial examples. *CoRR*, abs/1412.6572, 2014.
- Dan Hendrycks and Thomas Dietterich. Benchmarking neural network robustness to common corruptions and perturbations. In *International Conference on Learning Representations*, 2019.
- Dan Hendrycks and Kevin Gimpel. Gaussian error linear units (gelus). *arXiv preprint arXiv:1606.08415*, 2016.
- Matt Jordan and Alexandros G Dimakis. Exactly computing the local lipschitz constant of relu networks. *Advances in Neural Information Processing Systems*, 33:7344–7353, 2020.
- Guy Katz, Clark Barrett, David L Dill, Kyle Julian, and Mykel J Kochenderfer. Reluplex: An efficient smt solver for verifying deep neural networks. In *International Conference on Computer Aided Verification*, pp. 97–117. Springer, 2017.
- Hyunjik Kim, George Papamakarios, and Andriy Mnih. The lipschitz constant of self-attention. In *International Conference on Machine Learning*, pp. 5562–5571. PMLR, 2021.
- Pang Wei Koh, Shiori Sagawa, Henrik Marklund, Sang Michael Xie, Marvin Zhang, Akshay Balsubramani, Weihua Hu, Michihiro Yasunaga, Richard Lanus Phillips, Irena Gao, et al. Wilds: A benchmark of in-the-wild distribution shifts. In *International Conference on Machine Learning*, pp. 5637–5664. PMLR, 2021.
- Daniel Kuhn, Peyman Mohajerin Esfahani, Viet Anh Nguyen, and Soroosh Shafieezadeh-Abadeh. Wasserstein distributionally robust optimization: Theory and applications in machine learning. In *Operations Research & Management Science in the Age of Analytics*, Tutorials in Operations Research, pp. 130–166. INFORMS, 2019.

- Alexey Kurakin, Ian J Goodfellow, and Samy Bengio. Adversarial examples in the physical world. In *Artificial intelligence safety and security*, pp. 99–112. Chapman and Hall/CRC, 2018.
- Chang Liu, Yinpeng Dong, Wenzhao Xiang, Xiao Yang, Hang Su, Jun Zhu, Yuefeng Chen, Yuan He, Hui Xue, and Shibao Zheng. A comprehensive study on robustness of image classification models: Benchmarking and rethinking. *Int. J. Comput. Vis.*, 133(2):567–589, February 2025.
- Ye Liu, Yaya Cheng, Lianli Gao, Xianglong Liu, Qilong Zhang, and Jingkuan Song. Practical evaluation of adversarial robustness via adaptive auto attack. In *Proceedings of the IEEE/CVF Conference on Computer Vision and Pattern Recognition*, pp. 15105–15114, 2022.
- Ze Liu, Yutong Lin, Yue Cao, Han Hu, Yixuan Wei, Zheng Zhang, Stephen Lin, and Baining Guo. Swin transformer: Hierarchical vision transformer using shifted windows. In *Proceedings of the IEEE/CVF International Conference on Computer Vision (ICCV)*, pp. 10012–10022, 2021.
- Aleksander Madry, Aleksandar Makelov, Ludwig Schmidt, Dimitris Tsipras, and Adrian Vladu. Towards deep learning models resistant to adversarial attacks. In *International Conference on Learning Representations*, 2018.
- Peyman Mohajerin Esfahani and Daniel Kuhn. Data-driven distributionally robust optimization using the wasserstein metric: Performance guarantees and tractable reformulations. *Mathematical Programming*, 171(1):115–166, 2018.
- Seyed-Mohsen Moosavi-Dezfooli, Alhussein Fawzi, and Pascal Frossard. Deepfool: a simple and accurate method to fool deep neural networks. In *Proceedings of the IEEE conference on computer vision and pattern recognition*, pp. 2574–2582, 2016.
- Vinod Nair and Geoffrey E Hinton. Rectified linear units improve restricted boltzmann machines. In *Proceedings of the 27th international conference on machine learning (ICML-10)*, pp. 807–814, 2010.
- Yaniv Ovadia, Emily Fertig, Jie Ren, Zachary Nado, David Sculley, Sebastian Nowozin, Joshua Dillon, Balaji Lakshminarayanan, and Jasper Snoek. Can you trust your model’s uncertainty? evaluating predictive uncertainty under dataset shift. *Advances in Neural Information Processing Systems*, 32, 2019.
- Alec Radford, Jeffrey Wu, Rewon Child, David Luan, Dario Amodei, and Ilya Sutskever. Language models are unsupervised multitask learners. *OpenAI blog*, 1(8):9, 2019.
- Prajit Ramachandran, Barret Zoph, and Quoc V Le. Searching for activation functions. *arXiv preprint arXiv:1710.05941*, 2017.
- Leslie Rice, Anna Bair, Huan Zhang, and J Zico Kolter. Robustness between the worst and average case. In A. Beygelzimer, Y. Dauphin, P. Liang, and J. Wortman Vaughan (eds.), *Advances in Neural Information Processing Systems*, 2021.
- Jérôme Rony, Luiz G Hafemann, Luiz S Oliveira, Ismail Ben Ayed, Robert Sabourin, and Eric Granger. Decoupling direction and norm for efficient gradient-based l2 adversarial attacks and defenses. In *Proceedings of the IEEE/CVF conference on computer vision and pattern recognition*, pp. 4322–4330, 2019.
- Hadi Salman, Jerry Li, Ilya Razenshteyn, Pengchuan Zhang, Huan Zhang, Sebastien Bubeck, and Greg Yang. Provably robust deep learning via adversarially trained smoothed classifiers. *Advances in Neural Information Processing Systems*, 32, 2019.
- Filippo Santambrogio. *Optimal transport for applied mathematicians*. Springer, 2015.
- Vikash Sehwal, Saeed Mahloujifar, Tinashe Handina, Sihui Dai, Chong Xiang, Mung Chiang, and Prateek Mittal. Robust learning meets generative models: Can proxy distributions improve adversarial robustness? In *International Conference on Learning Representations*, 2022.
- Zhouxing Shi, Yihan Wang, Huan Zhang, J Zico Kolter, and Cho-Jui Hsieh. Efficiently computing local lipschitz constants of neural networks via bound propagation. *Advances in Neural Information Processing Systems*, 35:2350–2364, 2022.

- Gagandeep Singh, Timon Gehr, Matthew Mirman, Markus Püschel, and Martin Vechev. Fast and effective robustness certification. *Advances in Neural Information Processing Systems*, 31, 2018.
- Naman Deep Singh, Francesco Croce, and Matthias Hein. Revisiting adversarial training for imagenet: Architectures, training and generalization across threat models. In *Thirty-seventh Conference on Neural Information Processing Systems*, 2023.
- Christian Szegedy, Wojciech Zaremba, Ilya Sutskever, Joan Bruna, Dumitru Erhan, Ian Goodfellow, and Rob Fergus. Intriguing properties of neural networks. In *2nd International Conference on Learning Representations, ICLR 2014*, 2014.
- Rohan Taori, Achal Dave, Vaishaal Shankar, Nicholas Carlini, Benjamin Recht, and Ludwig Schmidt. Measuring robustness to natural distribution shifts in image classification. *Advances in Neural Information Processing Systems*, 33:18583–18599, 2020.
- Yusuke Tashiro, Yang Song, and Stefano Ermon. Diversity can be transferred: Output diversification for white- and black-box attacks. *Advances in Neural Information Processing Systems*, 33:4536–4548, 2020.
- Cédric Villani et al. *Optimal transport: old and new*, volume 338. Springer, 2008.
- Aladin Virmaux and Kevin Scaman. Lipschitz regularity of deep neural networks: analysis and efficient estimation. *Advances in Neural Information Processing Systems*, 31, 2018.
- Zekai Wang, Tianyu Pang, Chao Du, Min Lin, Weiwei Liu, and Shuicheng Yan. Better diffusion models further improve adversarial training. In *International Conference on Machine Learning*, pp. 36246–36263. PMLR, 2023.
- Lily Weng, Huan Zhang, Hongge Chen, Zhao Song, Cho-Jui Hsieh, Luca Daniel, Duane Boning, and Inderjit Dhillon. Towards fast computation of certified robustness for relu networks. In *International Conference on Machine Learning*, pp. 5276–5285. PMLR, 2018.
- Eric Wong and Zico Kolter. Provable defenses against adversarial examples via the convex outer adversarial polytope. In *International Conference on Machine Learning*, pp. 5286–5295. PMLR, 2018.
- Ruibin Xiong, Yanyan Yang, Di He, Kai Zheng, Shuxin Zheng, Chen Xing, Huishuai Zhang, Yanyan Lan, Liwei Wang, and Tie-Yan Liu. On layer normalization in the transformer architecture. In *International Conference on Machine Learning (ICML)*, pp. 10524–10533. PMLR, 2020.
- Xiaoyun Xu, Shujian Yu, Zhuoran Liu, and Stjepan Picek. Mimir: Masked image modeling for mutual information-based adversarial robustness. *arXiv preprint arXiv:2312.04960*, 2025. Accepted by NDSS 2026.
- Yuancheng Xu, Yanchao Sun, Micah Goldblum, Tom Goldstein, and Furong Huang. Exploring and exploiting decision boundary dynamics for adversarial robustness. In *The Eleventh International Conference on Learning Representations*, 2023.
- Huan Zhang, Shiqi Wang, Kaidi Xu, Yihan Wang, Suman Jana, Cho-Jui Hsieh, and Zico Kolter. A branch and bound framework for stronger adversarial attacks of relu networks. In *International Conference on Machine Learning*, pp. 26591–26604. PMLR, 2022.

A PRELIMINARIES ON WDRO

Recall that given two probability measures \mathbb{P} and \mathbb{Q} on \mathcal{Z} , the Wasserstein distance is defined as

$$\mathcal{W}_{d,p}(\mathbb{P}, \mathbb{Q}) \triangleq \left(\inf_{\pi \in \Pi(\mathbb{P}, \mathbb{Q})} \int_{\mathcal{Z} \times \mathcal{Z}} d^p(z', z) d\pi(z', z) \right)^{1/p}$$

for $p \in [1, \infty)$, and $\mathcal{W}_{d,p}(\mathbb{P}, \mathbb{Q}) \triangleq \inf_{\pi \in \Pi(\mathbb{P}, \mathbb{Q})} \text{ess. sup}_{\pi}(d)$ for $p = \infty$, where the feasible set is given by

$$\Pi(\mathbb{P}, \mathbb{Q}) \triangleq \{ \pi \text{ on } \mathcal{Z} \times \mathcal{Z} \mid \pi(A \times \mathcal{Z}) = \mathbb{P}(A), \pi(\mathcal{Z} \times B) = \mathbb{Q}(B) \forall A, B \subseteq \mathcal{Z} \}$$

the set of couplings (transport plans) between \mathbb{P} and \mathbb{Q} . Intuitively, a transportation plan π is feasible if it is a joint distribution whose first marginal is \mathbb{P} and second marginal \mathbb{Q} . In the ambiguity set $\Omega_p = \{ \mathbb{P} \mid \mathcal{W}_{d,p}(\mathbb{P}, \mathbb{P}_N) \leq \epsilon \}$ of problem equation 3, a (distributional) attack \mathbb{P} is admissible if the minimal effort for moving mass from \mathbb{P} to the empirical distribution \mathbb{P}_N is not exceeding budget ϵ . Unlike traditional approaches which only allows point-wise perturbations, WDRO min-max model equation 3 allows both discrete and continuous distribution \mathbb{P} , which is extremely practical in certain scenarios where the ground-truth distribution \mathbb{P}_{true} is unknown and possibly continuous.

B PROOFS OF MAIN RESULTS

B.1 PROOF OF THEOREM 3.1

Proof of Upper Bound. It is a standard result that for any $y = e_k$, if ℓ is the cross-entropy loss then

$$\begin{aligned} |\ell(x', y; \theta) - \ell(x, y; \theta)| &= |\log(\text{softmax } \theta(x'))_k - \log(\text{softmax } \theta(x))_k| \\ &\leq 2^{1/r} \|\theta(x') - \theta(x)\|_s, \end{aligned} \quad (12)$$

or if ℓ is the DLR loss then

$$\begin{aligned} |\ell(x', y; \theta) - \ell(x, y; \theta)| &= |(\max_{k_1 \neq k} \theta(x')_{k_1} - \theta(x')_k) - (\max_{k_2 \neq k} \theta(x)_{k_2} - \theta(x)_k)| \\ &\leq 2^{1/r} \|\theta(x') - \theta(x)\|_s. \end{aligned} \quad (13)$$

In addition, by Jordan & Dimakis (2020), we have that for any $x', x \in \mathcal{X}$,

$$\|\theta(x') - \theta(x)\|_s \leq \max_{\mathcal{D} \in \mathcal{D}_{\mathcal{X}}} \|J_{\mathcal{D}}\|_{r \rightarrow s} \times \|x' - x\|_r. \quad (14)$$

Thus,

$$\begin{aligned} |\ell(x', y; \theta) - \ell(x, y; \theta)| &\leq 2^{1/r} \max_{\mathcal{D} \in \mathcal{D}_{\mathcal{X}}} \|J_{\mathcal{D}}\|_{r \rightarrow s} \times \|x' - x\|_r \\ &= \mathbf{L} \times d((x', y), (x, y)). \end{aligned} \quad (15)$$

for any $x', x \in \mathcal{X}$ and therefore by using Lipschitz certificate (Mohajerin Esfahani & Kuhn, 2018; Blanchet et al., 2019; Gao & Kleywegt, 2023; Gao et al., 2024; Chu et al., 2024), we have

$$\sup_{\mathbb{P}: \mathcal{W}_{d,1}(\mathbb{P}, \mathbb{P}_N) \leq \epsilon} \mathbb{E}_{\mathbb{P}}[\ell(Z; \theta)] \leq \mathbb{E}_{\mathbb{P}_N}[\ell(Z; \theta)] + \mathbf{L}\epsilon, \quad (16)$$

for any $\epsilon > 0$.

Proof of Lower Bound. To show that the lower bound of the worst-case loss is $\mathbb{E}_{\mathbb{P}_N}[\ell(Z; \theta)] + \mathbf{l}\epsilon$, it is enough to construct a perturbation \tilde{Z} , a weight $\eta \in (0, 1]$, and a distribution

$$\mathbb{P}_{\text{adv}} = \sum_{i=1, i \neq \iota}^N \frac{1}{N} \delta_{Z^{(\iota)}} + \frac{1-\eta}{N} \delta_{Z^{(\iota)}} + \frac{\eta}{N} \delta_{\tilde{Z}}, \quad (17)$$

so that $\mathcal{W}_{d,1}(\mathbb{P}_{\text{adv}}, \mathbb{P}_N) \leq \epsilon$ and $\mathbb{E}_{\mathbb{P}_{\text{adv}}}[\ell(Z; \theta)] \approx \mathbb{E}_{\mathbb{P}_N}[\ell(Z; \theta)] + \mathbf{l}\epsilon$.

Since $\mathcal{D}_{\mathcal{X}}$ is finite, let x^* , \mathbf{D}^* , k'^* , k^* and sequence $\{u_t^*\}$ be the maximizer in equation 7, i.e., $\mathbf{D}^* \in \mathcal{D}_{x^*}$, $k'^* \neq k^*$, $\{u_t^*\} \subset \text{int}(\text{rec}(\mathcal{C}_{\mathbf{D}^*}))$ and

$$(e_{k'^*} - e_{k^*})^\top J_{\mathbf{D}^*} u_t^* \rightarrow \mathbf{l} \text{ when } t \rightarrow \infty.$$

In particular, θ is affine and differentiable on $\text{rec}(\mathcal{C}_{D^*})$. Since u_t^* belongs to the open cone $\text{rec}(\mathcal{C}_{D^*})$, one has that for any $\alpha > 0$,

$$\tilde{x} = x^* + \alpha u_t^* \in \text{rec}(\mathcal{C}_{D^*}), \quad (18)$$

and thus

$$\nabla_x \theta(\tilde{x}) = J_{D^*}, \quad \theta(\tilde{x}) - \theta(x^*) = \alpha J_{D^*} u_t^*. \quad (19)$$

Choose root ι so that $(X^{(\iota)}, Y^{(\iota)}) = e_{k^*}$. Then when ℓ is the cross-entropy loss or DLR loss, by a technical Lemma C.1 one has

$$\lim_{\alpha \rightarrow \infty} \frac{\Delta \ell(\alpha)}{\alpha} = \lim_{\alpha \rightarrow \infty} \frac{\ell(\tilde{x}, Y^{(\iota)}; \theta) - \ell(x^*, Y^{(\iota)}; \theta)}{\alpha} \geq v_{k'^*} - v_{k^*}. \quad (20)$$

where $v = J_{D^*} u_t^*$. Now choose α large enough so that $\Delta \ell(\alpha) \approx \alpha(v_{k'^*} - v_{k^*})$, $\Delta \ell(\alpha) \gg \ell(x^*, Y^{(\iota)}; \theta) - \ell(X^{(\iota)}, Y^{(\iota)}; \theta)$, and $N\epsilon < \|\tilde{x} - X^{(\iota)}\|_r \approx \alpha$. Set $\tilde{Z} = (\tilde{x}, Y^{(\iota)})$, then

$$\begin{aligned} \ell(\tilde{Z}; \theta) - \ell(Z^{(\iota)}; \theta) &= \Delta \ell(\alpha) + \ell(x^*, Y^{(\iota)}; \theta) - \ell(X^{(\iota)}, Y^{(\iota)}; \theta) \\ &\approx \|\tilde{x} - X^{(\iota)}\|_r (v_{k'^*} - v_{k^*}) \\ &= d(\tilde{Z}, Z^{(\iota)}) \times (e_{k'^*} - e_{k^*})^\top J_{D^*} u_t^* \xrightarrow{t \rightarrow \infty} \mathbf{l} \times d(\tilde{Z}, Z^{(\iota)}). \end{aligned} \quad (21)$$

Now set $\eta = \frac{N\epsilon}{d(\tilde{Z}, Z^{(\iota)})} \in (0, 1]$, then

$$\mathcal{W}_{d,1}(\mathbb{P}_{\text{adv}}, \mathbb{P}_N) \leq \frac{\eta}{N} d(\tilde{Z}, Z^{(\iota)}) = \epsilon. \quad (22)$$

Moreover,

$$\begin{aligned} \mathbb{E}_{\mathbb{P}_{\text{adv}}}[\ell(Z; \theta)] &= \mathbb{E}_{\mathbb{P}_N}[\ell(Z; \theta)] + \frac{\eta}{N} \left(\ell(\tilde{Z}; \theta) - \ell(Z^{(\iota)}; \theta) \right) \\ &\approx \mathbb{E}_{\mathbb{P}_N}[\ell(Z; \theta)] + \frac{\epsilon}{d(\tilde{Z}, Z^{(\iota)})} \mathbf{l} d(\tilde{Z}, Z^{(\iota)}) \\ &= \mathbb{E}_{\mathbb{P}_N}[\ell(Z; \theta)] + \mathbf{l}\epsilon. \end{aligned} \quad (23)$$

Therefore, the lower bound of the worst-case loss is $\mathbb{E}_{\mathbb{P}_N}[\ell(Z; \theta)] + \mathbf{l}\epsilon$.

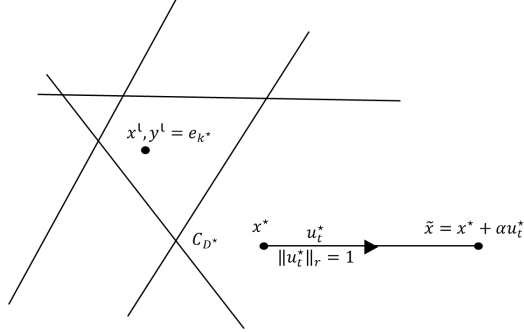


Figure 5: Illustration of Proof of Lower Bound

Sufficient condition of $\mathbf{l} = \mathbf{L}$. Suppose that the dual-norm maximizer $\xi = \mathcal{M}_r(J_{D^*}^\top (e_{k'^*} - e_{k^*})) \in \text{rec}(\mathcal{C}_{D^*})$ where D^* is a maximizer of equation 6 and (k'^*, k^*) is a maximizer of equation 7, then we have

$$\begin{aligned} \mathbf{l} &= (e_{k'^*} - e_{k^*})^\top J_{D^*} u_t^* \\ &\geq (e_{k'^*} - e_{k^*})^\top J_{D^*} \xi && \text{(since } u_t^* \text{ is the maximizer)} \\ &= \|(e_{k'^*} - e_{k^*})^\top J_{D^*}\|_s && \text{(by definition of dual-norm maximizer)} \\ &= \|(e_{k'^*} - e_{k^*})\|_r \|J_{D^*}\|_{r \rightarrow s} \\ &= 2^{1/r} \|J_{D^*}\|_{r \rightarrow s} = \mathbf{L}, \end{aligned} \quad (24)$$

where the second last equality holds true because $(e_{k'^*} - e_{k^*})$ is the largest increment direction of J_{D^*} .

B.2 PROOF OF THEOREM 3.3

Proof. The proof for the upper and lower bounds is similar to the methodology we discussed in our previous exchange.

Proof of Upper Bound. The WDRO upper bound is a direct consequence of the Lipschitz continuity of the loss function. The Lipschitz constant of the combined loss function, $L_\ell = \sup_{Z \in \mathcal{Z}} \|\nabla_x \ell(Z; \theta)\|_r$, is bounded by the product of the Lipschitz constant of the loss with respect to the output and the Lipschitz constant of the network. That is,

$$L \leq \|J_\theta(x)\|_{r \rightarrow s} \cdot \|\nabla \ell\|_s = \|J_\theta(x)\|_{r \rightarrow s} \cdot 2^{1/r}$$

Proof of Lower Bound. The proof of the lower bound is identical with the ReLU network case, where it relies on constructing a specific adversarial distribution. This finds a point x^* and a direction u^* that maximize the rate of change of the loss. The constant l is defined as this maximum rate of change. By constructing a perturbed point $\tilde{x} = x^* + \alpha u^*$ and a corresponding adversarial distribution, it is shown that the worst-case loss is at least $\mathbb{E}_{\mathbb{P}_N}[\ell(Z; \theta)] + l\epsilon$. \square

B.3 PROOF OF COROLLARY 3.4

Proof. Transformer blocks are compositions of differentiable primitives (linear maps, softmax attention, residual connections, LayerNorm with $\epsilon > 0$, and smooth activations), hence differentiable on \mathcal{X} . To obtain equation 10, one combines explicit Jacobian bounds for softmax self-attention from prior work (Kim et al., 2021; Castin et al., 2024) with standard Lipschitz calculus: for compositions, operator norms multiply (chain rule), and for residual maps $x \mapsto x + f(x)$ one has $\text{Lip}(\text{Id} + f) \leq 1 + \text{Lip}(f)$. Applying these rules block-by-block yields a product-form upper bound for $\sup_{x \in \mathcal{X}} |J_\theta(x)|_{2 \rightarrow 2}$, and the general $r \rightarrow s$ case follows from Hölder’s inequality. \square

C AUXILIARY RESULTS

Lemma C.1 (Asymptotics of loss). *If $\ell = \ell_{CE}$ is the cross-entropy loss in equation 20, then*

$$\lim_{\alpha \rightarrow \infty} \frac{\Delta \ell_{CE}}{\alpha} = \max_i (J_{\mathcal{D}^*} u_t^*)_i - (J_{\mathcal{D}^*} u_t^*)_{k^*}.$$

Else if $\ell = \ell_{DLR}$ is the DLR loss, then

$$\lim_{\alpha \rightarrow \infty} \frac{\Delta \ell_{DLR}}{\alpha} = \max_{i \neq k^*} (J_{\mathcal{D}^*} u_t^*)_i - (J_{\mathcal{D}^*} u_t^*)_{k^*}.$$

Proof. Let $\theta^* = \theta(x^*)$ and the change in network output be $\Delta \theta = \theta(\tilde{x}) - \theta(x^*) = \alpha J_{\mathcal{D}^*} u_t^*$. We will analyze the limit for each loss function separately.

Cross-Entropy Loss. The difference in loss is $\Delta \ell_{CE} = \ell_{CE}(\theta(\tilde{x}), e_{k^*}) - \ell_{CE}(\theta(x^*), e_{k^*})$. Using the property $\ell_{CE}(z, e_{k^*}) = -(z_{k^*} - \log \sum_k e^{z_k})$, the loss difference is:

$$\Delta \ell_{CE} = -\Delta \theta_{k^*} + \log \left(\sum_k e^{\Delta \theta_k} \cdot \text{softmax}(\theta^*)_k \right)$$

To find the limit of the average rate of change, $\frac{\Delta \ell_{CE}}{\alpha}$, we substitute $\Delta \theta = \alpha v$, where $v_k = (J_{\mathcal{D}^*} u_t^*)_k$.

$$\lim_{\alpha \rightarrow \infty} \frac{\Delta \ell_{CE}}{\alpha} = \lim_{\alpha \rightarrow \infty} \left[\frac{1}{\alpha} \log \left(\sum_k \text{softmax}(\theta^*)_k e^{\alpha v_k} \right) - v_{k^*} \right]$$

Let $v_{\max} = \max_k v_k$. Factoring out the dominant term $e^{\alpha v_{\max}}$ from the sum, the expression becomes:

$$= \lim_{\alpha \rightarrow \infty} \left[\frac{1}{\alpha} \left(\log(e^{\alpha v_{\max}}) + \log \left(\sum_k \text{softmax}(\theta^*)_k e^{\alpha(v_k - v_{\max})} \right) \right) - v_{k^*} \right]$$

$$= \lim_{\alpha \rightarrow \infty} \left[v_{\max} + \frac{1}{\alpha} \log \left(\sum_k \text{softmax}(\theta^*)_k e^{\alpha(v_k - v_{\max})} \right) - v_{k^*} \right]$$

The sum inside the logarithm converges to a constant value, as all terms with $v_k < v_{\max}$ go to 0. The logarithmic term is therefore bounded. The term $\frac{1}{\alpha}$ causes the entire second term to go to 0. The limit is thus:

$$= v_{\max} - v_{k^*} = \max_k (J_{\mathcal{D}^*} u_t^*)_k - (J_{\mathcal{D}^*} u_t^*)_{k^*}$$

DLR Loss. The difference in DLR loss is $\Delta \ell_{DLR} = \ell_{DLR}(\theta(\tilde{x}), k^*) - \ell_{DLR}(\theta(x^*), k^*)$.

$$\Delta \ell_{DLR} = \left(\max_{k \neq k^*} \theta(\tilde{x})_k - \theta(\tilde{x})_{k^*} \right) - \left(\max_{k \neq k^*} \theta(x^*)_k - \theta(x^*)_{k^*} \right)$$

Substituting $\theta(\tilde{x}) = \theta^* + \Delta\theta$:

$$\Delta \ell_{DLR} = \left(\max_{k \neq k^*} (\theta_k^* + \Delta\theta_k) - \max_{k \neq k^*} \theta_k^* \right) - \Delta\theta_{k^*}$$

To find the limit of the average rate of change, $\frac{\Delta \ell_{DLR}}{\alpha}$, we substitute $\Delta\theta = \alpha v$ and analyze as $\alpha \rightarrow \infty$.

$$\lim_{\alpha \rightarrow \infty} \frac{\Delta \ell_{DLR}}{\alpha} = \lim_{\alpha \rightarrow \infty} \frac{1}{\alpha} \left(\max_{k \neq k^*} (\theta_k^* + \alpha v_k) - \max_{k \neq k^*} \theta_k^* \right) - v_{k^*}$$

As $\alpha \rightarrow \infty$, the term αv_k dominates inside the maximum function. The limit of the maximum term is therefore $\max_{k \neq k^*} v_k$.

$$\lim_{\alpha \rightarrow \infty} \frac{\Delta \ell_{DLR}}{\alpha} = \left(\max_{k \neq k^*} v_k \right) - v_{k^*} = \max_{k \neq k^*} (J_{\mathcal{D}^*} u_t^*)_k - (J_{\mathcal{D}^*} u_t^*)_{k^*}$$

□

Corollary C.2 (Feasibility). Let $\mathbb{P}_N = \sum_{i=1}^N \mu_i \delta_{(x^{(i)}, y^{(i)})}$ and $d((x', y'), (x, y)) = \|x' - x\|_r + \infty \cdot \mathbf{1}_{\{y' \neq y\}}$. For $\alpha_i \in [0, 1]$ and points $\tilde{x}^{(i)} \in \mathcal{X}$, define

$$\mathbb{P}_{\text{adv}} \triangleq \sum_{i=1}^N \mu_i \left((1 - \alpha_i) \delta_{(x^{(i)}, y^{(i)})} + \alpha_i \delta_{(\tilde{x}^{(i)}, y^{(i)})} \right).$$

Then for any $p \in [1, \infty)$,

$$\mathcal{W}_{d,p}(\mathbb{P}_{\text{adv}}, \mathbb{P}_N)^p \leq \sum_{i=1}^N \mu_i \alpha_i \|\tilde{x}^{(i)} - x^{(i)}\|_r^p.$$

In particular, if $\sum_{i=1}^N \mu_i \alpha_i \|\tilde{x}^{(i)} - x^{(i)}\|_r^p \leq \epsilon^p$, then $\mathbb{P}_{\text{adv}} \in \Omega_p(\epsilon) = \{\mathbb{P} : \mathcal{W}_{d,p}(\mathbb{P}, \mathbb{P}_N) \leq \epsilon\}$.

Proof. Use the explicit coupling that leaves $(1 - \alpha_i)$ mass of each atom fixed and transports α_i mass from $(\tilde{x}^{(i)}, y^{(i)})$ to $(x^{(i)}, y^{(i)})$. □

D WDA STUDY

The κ parameter. Figure 6 illustrates how the robust accuracy of WDA varies as the parameter κ increases. Across all models, raising κ beyond 1 generally leads to a noticeable drop in robust accuracy. Specifically, for the models from Figure 6a in $r_2, \epsilon = 0.5$ settings, the best performance is observed at $\kappa = 3$, whereas for Ding et al. (2020); Cui et al. (2024); Wang et al. (2023); Sehwal et al. (2022) in Figure 6b, the lowest robust accuracy occurs at $\kappa = 2$. These results indicate that increasing κ can weaken model robustness, with the precise κ that produces the largest drop depending on the architecture.

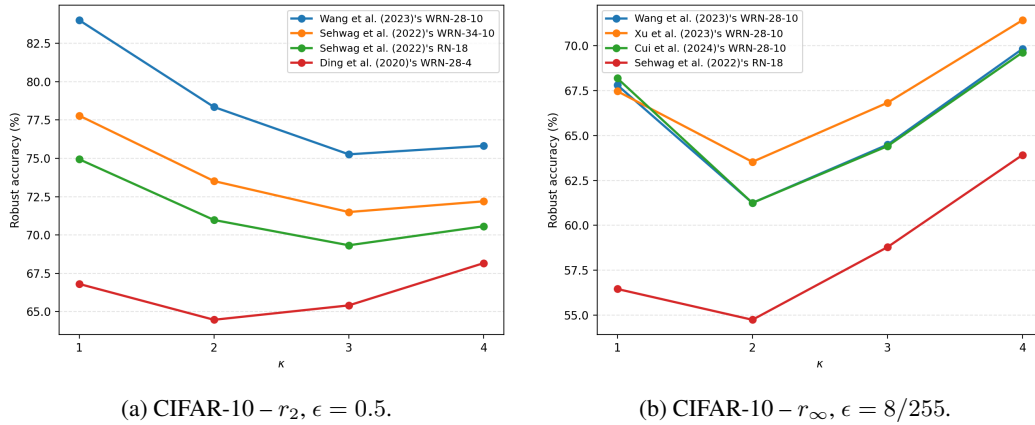


Figure 6: Analysis of robust accuracy across different κ scales.

The step size parameter. In Figure 7a ($r_2, \epsilon = 0.5$), we observe that step sizes significantly larger than the budget (e.g., 1.0 and 0.5) cause the fastest initial drop in accuracy but risk overshooting the optimal perturbation. In contrast, a moderate step size of 0.2 provides the most stable convergence to the lowest robust accuracy. Very small step sizes (0.01, 0.005) fail to explore the ϵ -ball effectively within the given iterations, resulting in an underestimation of the attack’s potency. Similarly, in Figure 7b ($r_\infty, \epsilon = 8/255 \approx 0.031$), the choice of step size is critical for convergence. A step size of 0.02 (approximately $2/3\epsilon$) yields the most potent attack. Step sizes significantly larger than ϵ (0.1, 0.5) lead to higher final robust accuracy due to oscillation around the boundary of the L_∞ ball, while the smallest step size (0.005) suffers from insufficient progress, failing to reach the floor within 20 iterations.

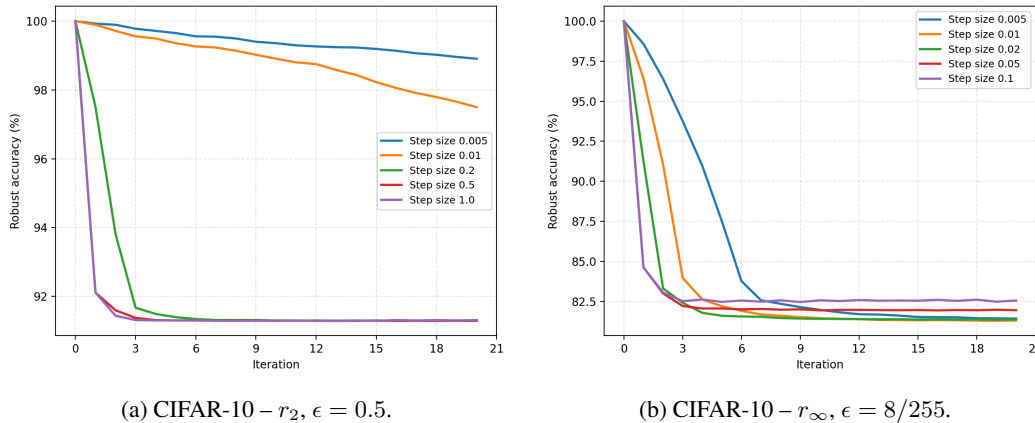


Figure 7: Analysis of convergence and step size effects across different perturbation types. (a) Method from Wang et al. (2023); (b) Method from Cui et al. (2024).

E WDA++ STUDY

While the standard WDA fixes a global scalar κ for all samples, WDA++ adopts an adaptive strategy to allocate the transport budget more efficiently. The core intuition is to assign higher transport mass (larger $1/\kappa_i$) to samples that are geometrically closer to the decision boundary, as these require less “cost” to flip. We report the classification accuracy on the constructed distribution \mathbb{P}_{adv} as

$$\frac{1}{N} \sum_{i=1}^N \left(1 - \frac{1}{\kappa_i} \right) \times \mathbf{1}_{\{h_\theta(x_i)=y_i\}} + \frac{1}{\kappa_i} \times \mathbf{1}_{\{h_\theta(x_i^{\text{adv}})=y_i\}},$$

where $h_\theta(x) = \arg \max_k \theta_k(x)$ is the class predictor. The practical implementation involves three specific algorithmic components to ensure efficiency and optimality under the budget constraint. These are detailed below and correspond to the steps in Algorithm 2.

Algorithm 2 WDA++

Inputs: neural network $\theta : \mathbb{R}^n \rightarrow \mathbb{R}^K$, empirical distribution $\mathbb{P}_N = \frac{1}{N} \sum_{i=1}^N \delta_{(X^{(i)}, Y^{(i)})}$, budget $\epsilon > 0$, cost-norm $r \in \{1, 2, \infty\}$, Wasserstein order $p \in \{1, 2\}$, step size $\alpha > 0$, `srchiter`, `maxiter`, and `topK`
Outputs: adversary distribution \mathbb{P}_{adv} such that $\mathcal{W}_{d,p}(\mathbb{P}_{\text{adv}}, \mathbb{P}_N) \leq \epsilon$, where $d((x', y'), (x, y)) = \|x' - x\|_r + \infty \cdot \mathbf{1}_{\{y' \neq y\}}$
Initialize: dual-norm maximizer \mathcal{M} equation 1
for $i = 1$ to N **do**
 if $\arg \max_{c \in \{1, \dots, K\}} \theta_c(x_0) \neq k$ **then** $X_{\text{adv}}^{(i)} \leftarrow X^{(i)}$, $d_i \leftarrow 0$ **continue**
 $x_0 \leftarrow X^{(i)}$
 $e_k \leftarrow Y^{(i)}$ for some $k \in \{1, \dots, K\}$
 $\mathcal{J}_i \leftarrow \arg \max_{\substack{\mathcal{J} \subseteq \{1, \dots, K\} \setminus \{k\} \\ |\mathcal{J}| = \text{topK}}} \sum_{j \in \mathcal{J}} \theta_j(x_0)$
 for `iter` = 0 to `maxiter` **do**
 $g_j \leftarrow \nabla_x \theta(x_{\text{iter}})^\top (e_j - e_k)$ for $j \in \mathcal{J}_i$
 $u_j \leftarrow \mathcal{M}_r(g_j)$ for $j \in \mathcal{J}_i$
 $\varphi_j \leftarrow x_{\text{iter}} + \alpha u_j$ for $j \in \mathcal{J}_i$
 $j^* \leftarrow \arg \max_{j \in \mathcal{J}_i} (\theta_j(\varphi_j) - \theta_k(\varphi_j))$
 $x_{\text{iter}+1} \leftarrow \varphi_{j^*}$
 if $\arg \max_{c \in \{1, \dots, K\}} \theta_c(x_{\text{iter}+1}) \neq k$ **then** $x_{\text{pre}}^{(i)} \leftarrow x_{\text{iter}}$, $x_{\text{flip}}^{(i)} \leftarrow x_{\text{iter}+1}$ **break**
 end for
 if $\arg \max_{c \in \{1, \dots, K\}} \theta_c(x_{\text{iter}+1}) = k$ **then** $X_{\text{adv}}^{(i)} \leftarrow X^{(i)}$, $d_i \leftarrow +\infty$ **continue**
 $\Delta \leftarrow x_{\text{flip}}^{(i)} - x_{\text{pre}}^{(i)}$, $t_\ell \leftarrow 0$, $t_u \leftarrow 1$
 for $j = 1$ to `srchiter` **do**
 $t \leftarrow (t_\ell + t_u)/2$
 $\tilde{x} \leftarrow x_{\text{pre}}^{(i)} + t\Delta$
 if $\arg \max_c \theta_c(\tilde{x}) \neq k$ **then** $t_u \leftarrow t$ **else** $t_\ell \leftarrow t$
 end for
 $X_{\text{adv}}^{(i)} \leftarrow x_{\text{pre}}^{(i)} + t_u \Delta$
 $d_i \leftarrow \|X_{\text{adv}}^{(i)} - X^{(i)}\|_r$
end for
 $\mathcal{I} \leftarrow \arg \text{sort}(\{d_i : i \in \{1, \dots, N\}\})$
 $\kappa_i \leftarrow +\infty$ for $i \in \{1, \dots, N\}$
 $B \leftarrow \epsilon^p$
for $i \in \mathcal{I}$ **do**
 if $B \leq 0$ **then break**
 $\kappa_i \leftarrow 1/\min\{1, NB/d_i^p\}$
 $B \leftarrow B - \frac{1}{N} \frac{1}{\kappa_i} d_i^p$
end for
 $\mathbb{P}_{\text{adv}} \leftarrow \frac{1}{N} \sum_{i=1}^N \left(1 - \frac{1}{\kappa_i}\right) \delta_{(X^{(i)}, Y^{(i)})} + \frac{1}{\kappa_i} \delta_{(X_{\text{adv}}^{(i)}, Y^{(i)})}$
return \mathbb{P}_{adv}

Direction search via Top-K heuristic. Evaluating the gradient for all $K - 1$ target classes can be computationally expensive for datasets with many classes (e.g., CIFAR-100, ImageNet). To accelerate the attack, we employ a `topK` heuristic. We restrict the search for the optimal adversarial direction to the top- K classes with the highest logits (excluding the correct class). In our experiments, we set `topK` = 20 for ImageNet, `topK` = 10 for CIFAR-100 and `topK` = 5 for CIFAR-10.

Boundary estimation via binary search. To compute the minimal flip cost, we cannot rely solely on the gradient step, as it may overshoot or undershoot the decision boundary. Instead, we perform a binary search along the direction of the successful perturbation vector $\Delta = x_{\text{flip}}^{(i)} - x_{\text{pre}}^{(i)}$. This refinement step, controlled by `srchiter` = 10, gives d_i .

Budget allocation. WDA++ adaptively allocates the global Wasserstein budget ϵ by treating the attack as a Knapsack-like optimization problem: maximizing misclassified samples subject to

$\sum \mu_i d_i^p / \kappa_i \leq \epsilon^p$. We adopt an optimal greedy strategy that calculates the flip cost d_i for each sample, sorts them in ascending order, and sequentially assigns maximum weight (up to $\kappa_i = 1$) to the “cheapest” samples until the budget $B = \epsilon^p$ is exhausted. This prioritizes the weakest links in the model to maximize the error rate for a given distributional radius.